

# Improving Video Instance Segmentation via Temporal Pyramid Routing

Xiangtai Li<sup>1\*</sup>, Hao He<sup>2,3\*</sup>, Henghui Ding<sup>4</sup>, Kuiyuan Yang<sup>6</sup>,  
Guangliang Cheng<sup>5</sup>, Jianping Shi<sup>5</sup>, Yunhai Tong<sup>1</sup>

<sup>1</sup> Key Laboratory of Machine Perception (MOE), Peking University

<sup>2</sup> NLPR, Institute of Automation, Chinese Academy of Sciences

<sup>3</sup> School of Artificial Intelligence, University of Chinese Academy of Sciences

<sup>4</sup> Nanyang Technological University <sup>5</sup> SenseTime Research <sup>6</sup> DeepMotion

## Abstract

Video Instance Segmentation (VIS) is a new and inherently multi-task problem, which aims to detect, segment and track each instance in a video sequence. Existing approaches are mainly based on single-frame features or single-scale features of multiple frames, where temporal information or multi-scale information is ignored. To incorporate both temporal and scale information, we propose a Temporal Pyramid Routing (TPR) strategy to conditionally align and conduct pixel-level aggregation from a feature pyramid pair of two adjacent frames. Specifically, TPR contains two novel components, including Dynamic Aligned Cell Routing (DACR) and Cross Pyramid Routing (CPR), where DACR is designed for aligning and gating pyramid features across temporal dimension, while CPR transfers temporally aggregated features across scale dimension. Moreover, our approach is a plug-and-play module and can be easily applied to existing instance segmentation methods. Extensive experiments on YouTube-VIS dataset demonstrate the effectiveness and efficiency of the proposed approach on several state-of-the-art instance segmentation methods. Codes and trained models will be publicly available to facilitate future research. (<https://github.com/lxtGH/TemporalPyramidRouting>).

## 1. Introduction

Instance segmentation is one of the fundamental vision tasks and has achieved significant progress in the image domain using deep convolution networks [26, 7, 11, 9, 55, 13, 61]. Recently, Video Instance Segmentation (VIS) [69], *i.e.*, instance segmentation in the video domain, has been proposed and drawn lots of attention. VIS aims to simultaneously classify, segment and track object instances in a

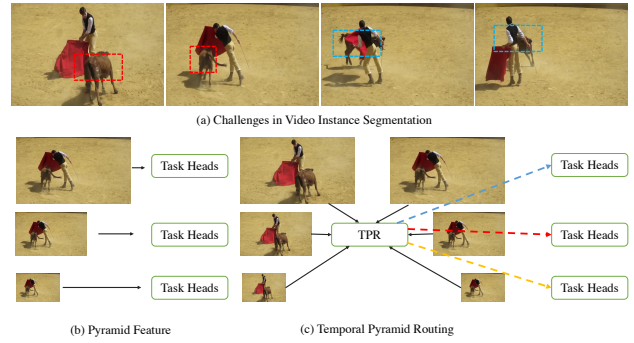


Figure 1: (a) The illustration of problems in video instance segmentation: scale variation (red boxes) and overlapping (blue boxes). (b) Pyramid feature learning in image understand tasks. (c) Our proposed Temporal Pyramid Routing. Each line in a different color represents per-pixel-wise routing across different scales along the temporal dimension.

given video sequence. It is a very challenging task that involves the instance correlations along the temporal dimension, which requires tracking across consecutive frames, besides the instance segmentation in each frame.

Previously, many state-of-the-art methods [4, 62] model the temporal correlation by feature aggregation. For example, Mask-Prop [4] proposes to warp mask features via a strong object detector [12] while VisTR [62] treats the entire video clips as sequence inputs and aggregates features via the transformer detector [10]. Moreover, bottom-up methods [67, 2] adopt separate object instances by clustering learned pixel embeddings [43] and then perform tracking and association via specific post-processing. However, these methods pay little attention to the scale variation problems when modeling temporal feature aggregation, resulting in ambiguous predictions for large variation objects. As shown in Fig. 1(a), the cow in one video clip has a large-scale variation between frames. To segment and track ob-

\*The first two authors contribute equally. Email: lxtpku@pku.edu.cn.

jects consistently across consecutive frames in a video, it is essential to incorporate past context and feature pyramids through a temporal model.

The scale variation problems have been well studied in the image domain via pyramid representation as shown in Fig. 1(b). Feature Pyramid Network (FPN) [36, 37, 26] and its variants [41, 23, 54] are the most classic architectures to establish a pyramid network for object representation. It assigns instances to different pyramid levels according to the object sizes. However, it has not been well explored in the video by how to align other feature pyramids across the different feature levels along the temporal dimension. Also, it has not been well studied on how to model the spatial-temporal feature pyramids for the down-stream tasks. Several works utilize optical flow [75, 74, 40] or non-local operators [14, 22] to aggregate temporal features for video object detection task. However, both limited scale variation and simple scenario on ImageNet VID dataset [51] make current methods mainly focus on single scale feature aggregation using Faster R-CNN [50] as the baseline. In this work, we aim to design an approach that enhances the network’s ability to handle the video domain’s scale variation problem.

Directly fusing the previous feature pyramid into the corresponding feature pyramid is a trivial solution because there may be significant motion variation and background noise in the video. Thus masking irrelevant features and dynamically assigning relevant parts in the previous frame is essential for temporal consistent feature representation. However, existing warping-based approaches [74, 72, 14] may lead to high computation costs. Inspired by the success of dynamic routing design in image tasks [53, 34], we propose a conceptually novel method for fine-grained temporal feature learning, called Temporal Pyramid Routing (TPR) which dynamically aligns and fuses features, performs pixel-wise routing between adjacent feature pyramids. As shown in Fig. 1(c), our TPR takes two adjacent temporal feature pyramids as input and outputs refined feature pyramids for the down-stream task. In particular, we design a novel pyramid routing space that mainly contains two steps: Dynamic Aligned Cell Routing and Cross Pyramid Routing. The former uses specifically designed double gates to filter out background noise and absorb relevant semantics. The latter introduces the aligned features from the previous frame into the remaining scales dynamically and efficiently. Fig. 2 gives a visual example of the TPR inference procedure. For each pyramid feature, only highlight parts from the previous frame are propagated into the current frame via pixel-level routing. Finally, we verify our proposed TPR on various baselines [11, 9, 7] on YouTube-VIS dataset [69]. The experimental results show that our proposed TPR improves baselines by a significant margin (about 2%-3% mAP) with little extra GFlops.

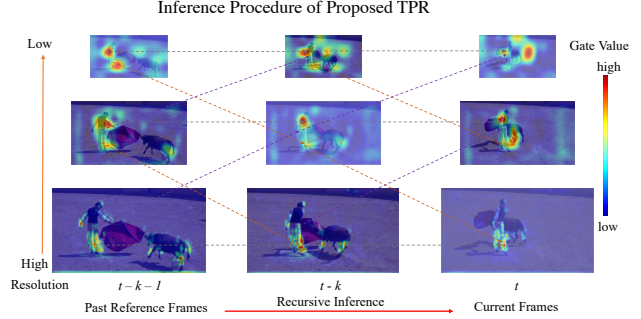


Figure 2: An illustration of the inference procedure of our proposed TPR. Only parts of feature (highlighted by gates) are propagated into the next frame sparsely and recursively.

Overall, the proposed TPR is fundamentally different from existing feature aggregation methods in video. TPR has utilized fine-grained feature representation via pixel-wise gated routing while maintaining inference efficiency while previous works [14, 74] introduce much more computation and redundant information between the frames. In summary, our main contributions are summarized as follows:

- 1) We propose a novel framework named Temporal Pyramid Routing for temporal dynamic multi-scale representation learning. In particular, we design two main components including Dynamic Aligned Cell Routing and Cross Pyramid Routing to aggregate features from the previous frame while keeping efficiency.
- 2) Our TPR is a plug-in module and we append our TPR into several image instance segmentation methods to perform temporal dynamic routing for VIS task.
- 3) Detailed experiments and analyses on the YouTube-VIS dataset indicate our proposed TPR’s efficacy in improving the accuracy and keeping light-weight. Our method improves baselines by a significant margin.

## 2. Related Work

**Image Instance Segmentation** Instance Segmentation aims to detect and segment each instance [16, 25]. The two-stage pipeline Mask-RCNN and its variants [26, 30, 12] first generate object proposals using Region Proposal Network (RPN) [50] and then predict boxes and masks on each RoI feature. Recently, several single-stage methods [13, 55, 11, 7, 61] achieve significant progress and comparable results with two-stage pipelines. Meanwhile, there are several bottom-up approaches [43, 18, 42]. Our method is built on those top-down works and explores the correlation of the temporal feature pyramid.

**Video Object Segmentation (VOS)** VOS [47] is very close to VIS and it has two settings: unsupervised [58, 57] and semi-supervised [46, 59, 44]. The former segments a single

object while the latter tracks the first given mask. However, both settings ignore the semantic category of each object which is very different from VIS.

**Video Object Detection (VOD)** VOD aims at detecting objects in videos [51]. Recent works explore the temporal features consistency via feature warping and sampling [74, 72, 5] or non-local aggregation [28, 19, 14] to improve the robustness of the detection method [50]. However, the fixed architecture and heavy aggregation limit the application to VIS. Moreover, VIS requires association instance identities while VOD only considers per-frame detection.

**Video Object Tracking (VOT)** VOT can be viewed as one sub-task of video instance segmentation. Siamese-network-based trackers [6, 33, 32, 76] dominate the Single-Object Tracking (SOT) while most state-of-the-art Multi-Object Tracking (MOT) methods adopt the tracking-by-detection [21, 3, 63, 71] paradigm. Recently, Multi-Object Tracking and Segmentation (MOTS) task [60] is proposed to evaluate MOT along with instance segmentation. Due to its limited scale distribution and much fewer object categories, we do not compare it in this paper.

**Video Instance Segmentation** The VIS requires classifying, segmenting each instance for each frame, and assigning the same instance the same id. MaskTrack-RCNN [69] is the first attempt to address this task where they also propose YouTube-VIS dataset for benchmarking video instance segmentation algorithms. Maskprop [4] is built on state-of-the-art detection method HTC [12] and crops the extracted features via predicted masks, then propagates them temporally to improve the segmentation and tracking. Based on [69], the work [35] proposes modified variational autoencoder while CompFeat [22] aggregates both frame-level and object-level information. Recently, VisTR [62] solves VIS problem using detection transformer [10]. VIS is also closely related to video semantic segmentation [75], video panoptic segmentation [31] and its variants [64, 49].

**Dynamic Network Design** Several works design the specific dynamic components [68, 15, 1] and architectures [29] for image classification task where the parameters and architectures are conditioned on inputs. Recently, inspired by Neural Architecture Search (NAS) [39, 8, 48, 77], several works propose dynamic network design on dense pixel prediction tasks such as semantic segmentation [34] and object detection [53]. These methods have data-dependent routes which are adapted from the scale distribution of each input. Our methods are inspired by those works and we design a novel temporal dynamic routing strategy for the VIS task.

### 3. Method

In this section, we will first review dynamic routing for understanding static images. Then, we will present the proposed temporal pyramid routing for VIS and discuss its de-

sign principles. Finally, the overall framework is shown at the end of this section.

#### 3.1. Overview of Dynamic Routing in Image tasks

**Basic Notation and Concepts** Compared with static networks, dynamic networks [15, 34, 53] have larger network capacity and better results under certain budget constraints. In a dynamic network, a *routing space* is defined as *all potential paths*, and the routing process is to aggregate potential multi-scale features and choose routing paths conditioned on each input image using *cells* and *gates* in each path. *Cells* are the basic computation blocks while the *gates* control how much computation is performed conditionally for each input. Formally, given the input feature  $X_s^l \in \mathbb{R}^{C \times H \times W}$  with  $H \times W$  pixel-level locations and  $C$  channels, a cell processes the feature with an operation set  $\mathcal{O}$  contains widely-used network operators (e.g., convolutions, identity mapping),

$$H_s^l = \sum_{O^i \in \mathcal{O}} O^i(X_s^l) \quad (1)$$

where  $l$  means the current depth of routing space,  $s \in \{2^i, i = 3, 4, \dots, k\}$  denotes the feature scale,  $k$  is largest downsample ratio, in FCOS [56],  $k=7$ , namely P3, P4,...,P7. The output  $H_s^l$  is transferred to different scales according to the gating factor  $m_s^l$ . Take pixel-wised routing gates as an example, each pixel-level location has a gate factor generated by

$$m_s^l = G_s^l(X_s^l; \theta_s^l), \quad (2)$$

where  $\theta_s^l$  is the network parameters learned for defining the gating function  $G_s^l(\cdot)$ . The output  $m_s^l$  is normalized via a variant of the soft differentiable tanh function [53]. Finally,  $X_s^l$  is transformed into  $Y_s^l$  after going through a path formed by cells and gates, i.e.,

$$Y_s^l = H_s^l \cdot m_s^l. \quad (3)$$

In summary, Dynamic Routing controls the operators applied on an image via gates conditioned on the image content, which is different from NAS-based approaches [39, 77], where the network structure is only varied during training phase but fixed during inference.

**Motivation for Video Instance Segmentation** As shown in Fig. 1(a), a video is consisted of a sequence of images stacked along the temporal dimension. Comparing with a static image, a video contains more but redundant information, and also more variations caused by motion. Conditioned on a video input, dynamic routing is a natural mechanism to select useful instance information for VIS.

#### 3.2. Temporal Pyramid Routing

**Temporal Pyramid Dynamic Routing Space** The basic task for dynamic network is routing space design, which determines the potential capacity of the network. In this work,

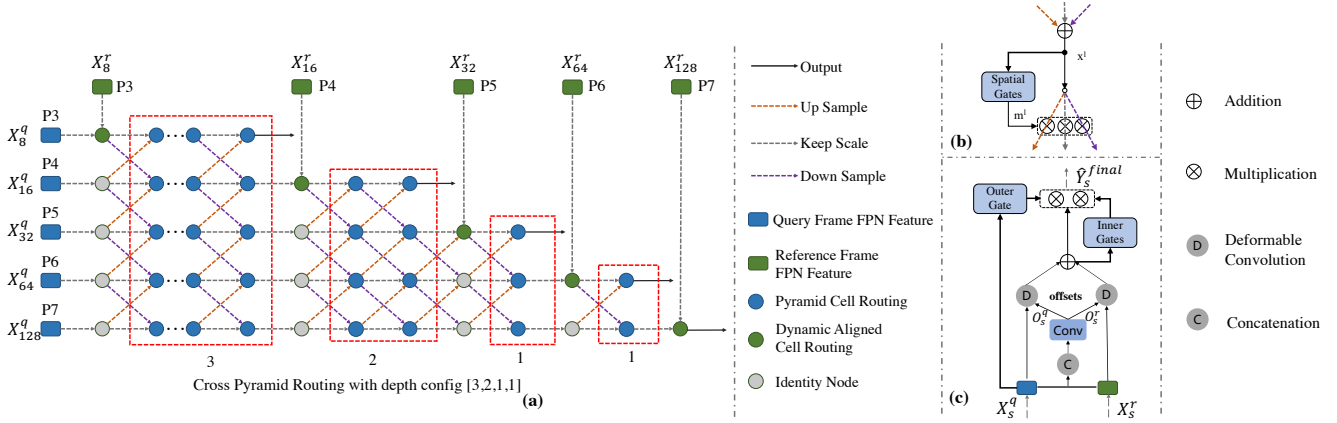


Figure 3: An illustration of our proposed Temporal Pyramid Routing system, which takes two feature pyramids as inputs (blue rectangles and green rectangles), and outputs the refined feature pyramids for down-stream tasks. Following VIS paper [69], Query frame represents the current frame while Reference frame is randomly sampled from the same video clip around current frame. (a) Overview of our TPR. It mainly contains two components: Dynamic Aligned Cell Routing (Green Circles) and Cross Pyramid Routing (Blue Circles in Red dotted boxes). (b) Detailed cell operation in Cross Pyramid Routing. (c) Detailed cell operation in Dynamic Aligned Cell Routing.

we use feature pyramid to represent multi-scale information of each frame, and feature pyramids from a video to capture temporal information. The routing space is designed to control the information flow along both temporal dimension and scale dimension. Feature pyramids go through the routing space, and are conditionally refined by selected paths. The whole routing process is defined as Temporal Pyramid Dynamic Routing (TPR). Finally, task-specific heads are attached to the refined feature pyramid for down-stream tasks, such as detection, segmentation and tracking. To be noted, it is a plug-and-play module which can be applied for any method using feature pyramid as input, which is also verified in Sec. 4.2.

As shown in Fig. 3(a), we take two feature pyramid inputs in one video sequence as an example. One feature pyramid  $X_s^q$  is from the query frame  $q$  (i.e., current frame, denoted as blue rectangles) and the other feature pyramid  $X_s^r$  is from the reference frame  $r$  (i.e., support frame, denoted as green rectangles). The input two feature pyramids goes through TPR, which routes temporal information via Dynamic Aligned Cell Routing (DACR) and scale information via Cross Pyramid Routing (CPR). DACR absorbs the most relevant information from reference frame in a pixel-wise manner scale by scale, while CPR routes the absorbed information to other scales. We will specify the designing details of these two components.

**Dynamic Aligned Cell Routing** As mentioned before, it is crucial to design a temporal pixel-wised routing cell to avoid noises and sample the most important parts. We adopt a sample and filter strategy to align temporal feature frames. First, Dynamic Aligned Cell Routing utilizes the dynamic

sampling operator [17] to sample corresponding pixel locations, and then irrelevant parts are filtered via our double gates design. Two features  $X_s^q(i)$  and  $X_s^r(i)$  are the inputs of our Dynamic Aligned Cell, where  $i$  is index of each spatial position. The first step is to find the correspondence between the two features. We concatenate two features and generate two individual offset fields  $O_s^r, O_s^q$  via one  $3 \times 3$  convolution layer. Then the correspondent features are sampled according to the predicted offset fields through deformable convolution (DCN) [17]. Take the query feature  $X_s^q(i)$  with predicted offset  $O_s^q$  as an example,

$$\hat{X}_s^q(i) = \sum_{p_n \in R} X_s^q(i + p_n + O_s^q(p_n)) \cdot W(p_n) \quad (4)$$

where  $p_n$  enumerates the locations in neighbor  $R$  and  $W$  is kernel weight of DCN. Then we perform pixel-wised dynamic routing using refined  $\hat{X}_s^q, \hat{X}_s^r$  and original  $X_s^q$  via our double gates.

There are two types of gate in DACR, i.e., inner gate and outer gate. Inner gate aims to control the sampled reference features and find fine-grained supports from reference features, while outer gate emphasizes informative locations in query frame and only absorb features from reference frames accordingly. In particular, for inner gates, we choose stride convolution and max-pooling for gate map generation to highlight the most salient areas. Following Equ. 3, the output of inner cell routing is formally defined as,

$$\hat{Y}_s = \{Y_s^i | Y_s^i = H_s^i \cdot Gate(Cat(\hat{X}_s^q, \hat{X}_s^r)), i \in q, r\} \quad (5)$$

where  $Cat$  means concatenation operation,  $Gate$  is the inner function, the hidden states  $H_s^i$  are generated by cell

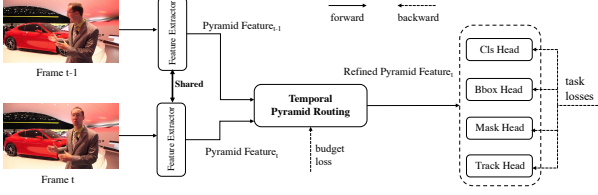


Figure 4: An illustration of network architecture with our proposed TPR. The feature extractor contains backbone and FPN. During inference, Frame  $t - 1$  is used as reference frame. Best view it on screen.

via Equ. 1. During inference, only pooled areas that are selected by the inner gate can be propagated into  $\hat{Y}_s^q$ , which can be efficiently implemented via masked convolution [24]. Finally, we fuse two features  $Y_s^q$  and  $Y_s^r$  via  $1 \times 1$  convolution, and denote the fusion result as  $Y_s^{merge}$  for short.

Although inner gates can be effective to avoid background noises, the contents are flexibly dependent on sampled offsets  $O_s^r, O_s^q$ , which affects the stability of the query frame feature learning. Thus we propose to combine query frame feature  $X_s^q$  and merged feature  $Y_s^{merge}$  via an outer gate map  $G_s$ . The gate map  $G_s$  is generated by convolutional fusion of  $X_s^q$  and  $Y_s^{merge}$  followed by a sigmoid function. Then, the final feature map is obtained as the weighted sum of  $X_s^q$  and  $Y_s^{merge}$  according  $G_s$ ,

$$\hat{Y}_s^{final} = G_s \cdot X_s^q + (1 - G_s) \cdot Y_s^{merge} \quad (6)$$

**Cross Pyramid Routing** After harvesting reference features from each scale  $s$ , the next important problem is how to distribute  $\hat{Y}_s^{final}$  to other scales of query feature pyramid. In FPN-like networks [36, 41], semantically strong features in low-resolution and semantically low features in high-resolution are combined in the network, which are also used in most state-of-the-art image instance segmentation approaches [11, 7, 9]. CPR follows the cross-scale, pixel-wised routing strategy [53] with two exceptions. One is the input feature that is modified by DACR. The other is the lower-triangular shaped routing space, where lower-level features go through deeper paths to upper-level features, to bridge the semantic gap therein. The default routing depth  $l$  is [3, 2, 1, 1] is used in all experiments, more choices about  $l$  can be found in the supplementary. The detailed procedure of each routing cell is shown in Fig. 3(b). Both DACR and CPR work at the same time for both training and inference.

**Discussion with Previous works** Compared with previous works using optical flow for warping features [75, 74], our dynamic network does not require the extra optical flow network training and adaption. Compared with DCN sampling [5], our proposed DACR can avoid background noises and achieve faster inference speed since only sparse locations are involved during the inference.

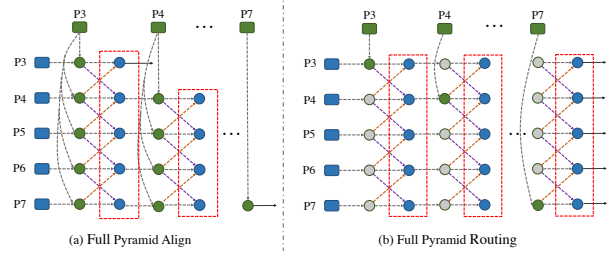


Figure 5: An illustration of more routing space designs. (a).Full pyramid align. (b).Full pyramid routing.

**Discussion on Routing Space Design** In addition to the proposed CPR design, there are another two straightforward design choices. One is Full Pyramid Align routing as illustrated in Fig. 5(a), where each node from reference feature pyramid is aligned to all nodes in the query feature pyramid via DACR. The other is Fully Pyramid Routing as proposed in [34], where all nodes in query feature pyramid are with the same routing depth. The former suffers from the severe misalignments between features across different scales. The latter treats all scales equally and leads to more redundant computations for upsampling high-level features.

### 3.3. Network Architectures

**Extending Image Instance Segmentation into Video VIS** requires the association of instances in a video. Following previous work [69, 9], we also add a tracking head for fair comparison shown in Fig. 4. The tracking head outputs feature embedding of each instance candidate. Suppose there are  $K$  instances identified from previous frames, the candidate box  $i$  in the current frame will be assigned to the label  $k$  according the assignment probability,

$$p_i(k) = \begin{cases} \frac{e^{f_i^T f_n}}{1 + \sum_{j=1}^K e^{f_i^T f_j}} & k \in [1, K] \\ \frac{1}{1 + \sum_{j=1}^K e^{f_i^T f_j}} & k = 0 \end{cases} \quad (7)$$

where  $1 \leq k \leq K$  indicates the candidate is associated to one of the  $K$  instances and  $k = 0$  means the candidate is treated as a new track,  $f_i$  and  $f_j$  ( $j \in [1, K]$ ) denote the feature embedding of the candidate and the  $K$  pre-identified instances, respectively. Then we adopt cross-entropy loss by treating it as a multi-class classification problem. As shown in Fig. 4, we insert our proposed TPR between feature extractor and these task-specific heads (detection, segmentation, tracking) for VIS.

**Loss function** Since the dynamic network has a large capacity while we only have limited computational resources, we constrain the computational cost by following previous works [34, 53], we consider all the locations involved in the receptive field of locations with positive gating factors, which are obtained by a max-pooling layer. We denote such computation budget from that gate as  $B^l$  for the layer  $l$ . The

budget loss is normalized by the overall computational complexity  $C^l$ .

$$\mathcal{L}_{\text{budget}} = \frac{\sum_l B^l}{\sum_l C^l} \quad (8)$$

Finally, the total loss  $\mathcal{L}$  is the combination of tasks-specific heads loss and budget loss. The positive hyper-parameters  $\lambda_1$  and  $\lambda_2$  are set to achieve a trade-off between efficiency and effectiveness, where we set  $\lambda_1 = 1$  and  $\lambda_2 = 1.5$  following [53] by default. The  $\mathcal{L}_{\text{tasks}}$  contains detection, segmentation and tracking loss,

$$\mathcal{L} = \lambda_1 \mathcal{L}_{\text{tasks}} + \lambda_2 \mathcal{L}_{\text{budget}}. \quad (9)$$

**Training and Inference** Following [69, 9], we train our network in a fair setting by randomly sampling one reference frame around the query frame. During inference, we adopt the online setting where only one previous reference frame is considered. Since our TPR can align the feature pyramid across temporal dimension, the reference frame also contains earlier cues in a recursive manner shown in Fig. 1(d). We adopt the same strategies for tracking heads as MaskTrack R-CNN [69] by maintaining a memory to store the feature vectors of existing instances.

## 4. Experiment

### 4.1. Implementation Details

**Dataset and Evaluation Metric** We evaluate our TPR on YouTube-VIS dataset [69], which has 2238 training, 302 validation, and 343 test videos. Each video is annotated with per-pixel segmentation, category, and instance ids. The dataset contains 40 object categories. Since only the validation set is available for evaluation, all results reported in this paper are evaluated on the validation set by uploading results to the online server. Following previous work, we adopt mAP proposed in [69] which are average precision (AP) and average recall (AR) based on a spatial-temporal Intersection-over-Union (IoU) as metrics. Both metrics adopt a COCO format where the AP is computed by averaging over multiple IoU thresholds (from 0.5 to 0.95). This metric considers all three tasks, including detection, segmentation, and tracking in a unified way. Since the dynamic network has different GFlops for different inputs, we report the average inference time (Frames Per Second, FPS) of all validation videos using one V-100 GPU card following [62]. Following [53], we also report different GFlops calculated on the validation set.

**Experiment Settings** We use the PyTorch library [45] and Detectron2 [66] to implement all the models. Following [69, 4], all the image instance segmentation models are pre-trained on COCO datasets [38]. We resize the original frame size to 640×360 for both training and testing. We

train all the models for 12 epochs. During training, the initial learning rate is set to 0.005 and decays with a factor of 10 after epoch 8 and 11. Multi-scale training is adopted to obtain a strong baseline. For each input frame, we randomly select two frames from the same video, one used as the query frame and the other used as the reference frame for training TPR and the tracking head. The reference frame is randomly sampled in a limited range of 3 for the query frame during training.

### 4.2. Experiments on YouTube-VIS

**Overview and Baseline** We will first perform ablation studies using BlendMask [11] with ResNet50 [27] backbone (with tracking head in Sec. 3.3) as the baseline to prove the effectiveness of our TPR. Then we will give a detailed analysis and further comparison of our TPR. In addition, we also report performance gain on several other instance segmentation methods [9, 7, 69]. Finally, we compare our methods with previous works at last.

**Ablation study for effectiveness of TPR** We first verify the effectiveness of each component in TPR in Tab. 1(a). Starting from the baseline model, we obtain 33.8% mAP. Adding DACR results in about 1.4 % mAP gain while CPR leads to 0.7 % mAP, which indicates temporal cues are more important. After combining both, there is a significant gain over the baseline by 2.1 % mAP. After using a strong baseline with ResNet101 as backbone, our TPR also has 2.5% mAP gain which proves scalability of our approach.

**Ablation study for DACR** In Tab. 1(b), we investigate the necessity of our essential modules for DACR design in Sec. 3.2. We progressively improve the baseline with: (1) DCN-based sampling in Equ. 4; (2) dynamic routing with inner gates in Equ. 5; (3) Outer gates fusion in Equ. 6. Consistent performance improvements can be observed after introducing the above modifications and we can draw two essential conclusions: (1) Both DCN-based sampled and dynamic routing can align features and have the same impact. However, combining both obtain better results. (2) Outer gates work complementary with the previous two and can further improve the performance.

**Ablation study for Cross Pyramid Routing Design** We give more routing space design comparison with our proposed Cross Pyramid Routing in Tab. 1(c). We conduct two different types of routing space design introduced in Sec. 3.2 and Fig. 5. Top-Down routing means we carry out routing from high-level features to low-level features and reverse the routing order of CPR. It results in inferior results since misalignment in low resolution is severer [52] and propagating such misaligned features into different scales hurts the performance for down-stream tasks. It also leads to more GFlops. The results indicate the effectiveness and efficiency of our CPR design and routing space design because all other designs will cause more misalignment across

Backbone	+ DACR	+ CPR	mAP(%)
ResNet50	-	-	33.8
ResNet50	✓	-	35.2
ResNet50	-	✓	34.5
ResNet50	✓	✓	35.9
ResNet101	-	-	36.6
ResNet101	✓	✓	39.1

(a) Effect of two main components on various baselines.

Method	Equ. 4	Equ. 5	Equ. 6	mAP(%)
Baseline				33.8
	✓			34.5
		✓		34.3
	✓	✓		34.8
	✓	✓	✓	35.2

(b) Effect of each component in DACR.

Settings	mAP(%)	$GFlops_{avg}$
baseline+DACR	35.2	58.9
+CPR	35.9	+2.3
+Full pyramid routing	35.0	+6.5
+Full pyramid align	33.4	+5.9
Top-Down routing(in CPR)	34.6	+4.8

(c) Ablation on routing space design under the same routing depth config. GFlops are measured on the entire validation set.

Sampling Method	mAP(%)
baseline + CPR	34.5
w DACR	35.9
w DCNv2 fusion [73]	35.2
w STSN [5]	35.1
w optical flow warp [75, 20]	35.0
w feature flow warp [40]	34.4

(d) Comparison other feature warp operations.(w: with)

Settings	mAP(%)
SipMask [9]	33.8
+Our TPR	35.9
YOACT [7]	32.3
+Our TPR	34.8
MaskTrack-RCNN [69]	30.2
+Our TPR	31.6

(e) Generation on other instance segmentation methods.

Method	Backbone	mAP(%)	$GFlops_{avg}$	$GFlops_{max}$	$GFlops_{min}$	Params
Baseline	ResNet50	33.8	56.8	56.8	56.8	41.2M
+TPR	ResNet50	35.9	+4.4	+4.9	+4.2	+10.2M
Baseline	ResNet101	36.6	75.7	75.7	75.7	60.1M
+TPR	ResNet101	39.1	+4.9	+6.1	+4.5	+14.2M

(f) Computation Analysis on various baselines. Both GFlops and parameters are reported. GFlops are measured on the entire validation set.

Table 1: **Ablation studies.** We first verify the effect of each module and design choices in the first row. Then we perform several comparison and analysis of our module in the second row. Due to the limited space, more implementation details can be in supplementary.

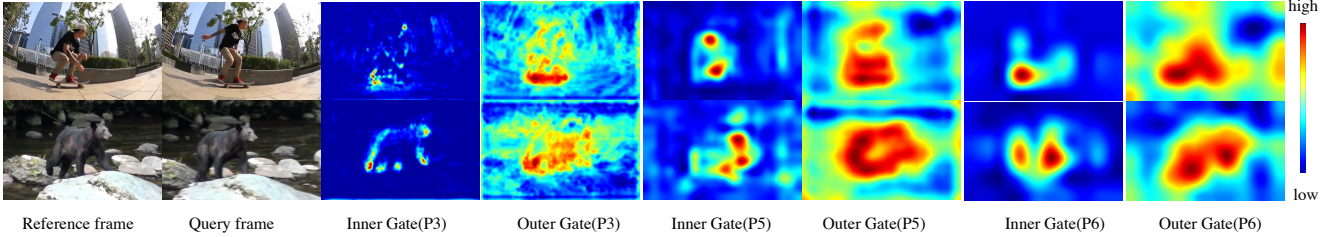


Figure 6: **Visualization of gates in Dynamic Aligned Cell Routing.** We choose three features (P3, P5, P6). The inner gates are all from the reference frame to control how much information is needed from the previous frame. The outer gates highlight the important regions in the current frame. Best view it on screen and Zoom in.

different scales and increase the ratio of misalignment parts for each feature pyramid while having more computation cost. The results verify our discussion in Sec. 3.2.

**Comparison with Warping-Based approaches** In Tab. 1(d), we give a further comparison with several feature warping-based approaches, including using optical flow like warping [74] and DCN-like warping [5]. We use the baseline method with our CPR for fair comparison. Compared with those works, our approach has the best result mainly because our proposed double gates can well propagate more relevant information.

#### Generation to More Instance Segmentation Approaches

We further generate our approaches on more methods, including SipMask [9], MaskTrack-RCNN [26] and YOACT [7]. All the methods use ResNet50 as backbone. As shown in Tab. 1(e), our TPR improves the results with considerable margins for different approaches. Note that all the methods are implemented in the same frame work under the same setting for fair comparison. More implementation details of these models can be found in supplementary.

**Computation Analysis** Since our method is dynamic and

it has different GFlops for different inputs. We report several different settings in Tab. 1(f) including the maximum GFlops, average GFlops and minimum GFlops. The results prove that our TPR can not only have fewer computational overhead but also improve performance by a large margin. For instance, our method obtains about 2.1%-2.5% relative mAP gains over the static baseline with a lower average computational complexity (relatively only about 6.4% - 7.7%). That indicates the potential of our approach for the application purpose.

#### Visualization of Gate Maps

In Fig. 6, we visualize several examples of our double gates. We observe that the inner gates mainly provide detailed and fine-grained instance details from the reference frame(such as heads or foot on beers) while the outer-gates focus on the current foreground objects(roughly location of instances in current frame). Both gates prohibit background noises and make the inference more efficient, which is consistent with our motivation in Sec. 1.

**Qualitative Results** In Fig. 7, we give two visual examples of the baseline method and our TPR with each group

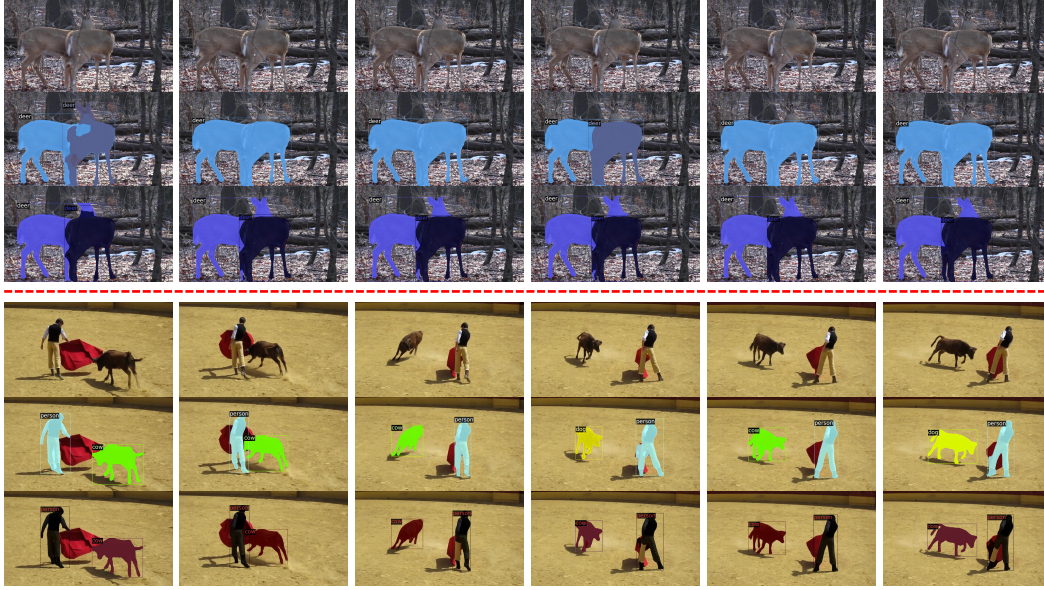


Figure 7: **Visualization results using our TPR on YouTube-VIS validation set.** Each row has five sampled frames from a video sequence. The first row for each video shows the original frames. The second row illustrates the mask predictions of Baseline Method(BlendMask with Tracking Head) and the third row those obtained with our TPR. Compared to baseline, our TPR tracks object instances more robustly even when they overlap with each other. Note that the same color represents the same object(id). Best view on the screen and zoom in.

Method	backbone	FPS	AP	AP <sub>50</sub>	AP <sub>75</sub>	AR <sub>1</sub>	AR <sub>10</sub>
DeepSORT [65]	ResNet50	-	26.1	42.9	26.1	27.8	31.3
FEELVOS [59]	ResNet50	-	26.9	42.0	29.7	29.9	33.4
OSMN [70]	ResNet50	-	27.5	45.1	29.1	28.6	33.1
MaskTrack R-CNN [69]	ResNet50	20.0	30.3	51.1	32.6	31.0	35.5
MaskProp[4]	ResNet50‡	< 2	40.0	-	42.9	-	-
MaskProp [4]	ResNet101‡	< 1	42.5	-	45.6	-	-
STEm-Seg [2]	ResNet50	-	30.6	50.7	33.5	31.6	37.1
STEm-Seg [2]	ResNet101	2.1	34.6	55.8	37.9	34.4	41.6
CompFeat [22]	ResNet50	-	35.3	56.0	38.6	33.1	40.3
VisTR [62]	ResNet50	30.0	34.4	55.7	36.5	33.5	38.9
VisTR [62]	ResNet101	27.7	35.3	57.0	36.2	34.3	40.4
BlendMask-baseline	ResNet50	19.3	33.4	52.8	36.1	32.7	38.0
<b>TPR-BlendMask</b>	ResNet50	16.1	35.9	56.8	38.9	35.2	41.6
SipMask-baseline	ResNet50	21.2	33.8	53.1	37.4	35.2	41.0
<b>TPR-SipMask</b>	ResNet50	15.3	35.9	57.0	36.8	36.2	43.6
<b>TPR-BlendMask</b>	ResNet101	10.1	39.1	59.1	43.4	38.8	45.6
<b>TPR-BlendMask</b>	ResNet101‡	8.2	40.5	60.4	44.7	39.8	46.0

Table 2: **Video instance segmentation AP (%)** on the YouTube-VIS [69] validation dataset. The compared methods are listed by publication date. Note that, for the first three methods, we use the results reported by the re-implementations in [69] for VIS. For BlendMask [11] and SipMask baselines [9], we report our re-implementation results for fair comparison. ‡means using DCN [17] in Backbone. The methods with underline are offline inference while the others are online inference.

containing images sampled from the same video. The same color represents the same instance identity. From these results, we observe that our TPR can segment instances well in two challenging situations: (1) instance overlapping (The

first group, two deers are very close with each other), (2) instance deformations and large variations (The second groups, the appearance of the cow has changed greatly over time, thus the cow is classified into the dog wrongly.). More results can be found in supplementary.

**Comparison the Previous Works** Finally, we give a detailed comparison on our methods with previous work in Tab. 2. The comparison contains several aspects, including accuracy, speed, inference type and backbone network. Though MaskProp [4] obtains higher mAP, that method is much slower. Moreover, MaskProp combines multiple networks such as video object detection network [5], Hybrid Task Cascade Network [12] for cascade feature learning and the complex High-Resolution Mask Refinement post-processing. Our method shares a much simpler pipeline and it can be a plug-in module to improve the video instance segmentation methods. As shown in the Tab. 2, our TPR improves the various models with little FPS drop. In particular, with ResNet101 and DCN [17] as backbone, our method can achieve **40.5 % mAP** while running at 8.2 FPS.

## 5. Conclusion

In this paper, we propose a conceptually new framework named Temporal Pyramid Routing (TPR) for dynamic instance learning in video. The pyramid features are well aligned and routed along the temporal dimension via TPR. In particular, we design specific Dynamic Aligned Cell

Routing (DACR) with a double gate design to avoid background noise while capturing useful information during the propagation. Moreover, the Cross Pyramid Routing (CPR) is proposed to propagate aligned features into all scales. Extensive experiments demonstrate the effectiveness and efficiency of our TPR on state-of-the-art instance segmentation methods on YouTube-VIS dataset where we achieve significant gains over the baselines. We hope this work can provide several insights into future works for modeling dynamics in video.

**Acknowledgement** Y. Tong is supported by the National Key Research and Development Program of China (No.2020YFB2103402).

## References

- [1] Amjad Almahairi, Nicolas Ballas, Tim Cooijmans, Yin Zheng, Hugo Larochelle, and Aaron Courville. Dynamic capacity networks. In *ICML*, 2016.
- [2] Ali Athar, Sabarinath Mahadevan, Aljoša Ošep, Laura Leal-Taixé, and Bastian Leibe. Stem-seg: Spatio-temporal embeddings for instance segmentation in videos. In *ECCV*, 2020.
- [3] Philipp Bergmann, Tim Meinhardt, and Laura Leal-Taixe. Tracking without bells and whistles. In *ICCV*, 2019.
- [4] Gedas Bertasius and Lorenzo Torresani. Classifying, segmenting, and tracking object instances in video with mask propagation. In *CVPR*, 2020.
- [5] Gedas Bertasius, Lorenzo Torresani, and Jianbo Shi. Object detection in video with spatiotemporal sampling networks. In *ECCV*, 2018.
- [6] Luca Bertinetto, Jack Valmadre, Joao F Henriques, Andrea Vedaldi, and Philip HS Torr. Fully-convolutional siamese networks for object tracking. In *ECCV*. Springer, 2016.
- [7] Daniel Bolya, Chong Zhou, Fanyi Xiao, and Yong Jae Lee. Yolact: Real-time instance segmentation. In *ICCV*, 2019.
- [8] Han Cai, Ligeng Zhu, and Song Han. Proxylessnas: Direct neural architecture search on target task and hardware. *arXiv preprint arXiv:1812.00332*, 2018.
- [9] Jiale Cao, Rao Muhammad Anwer, Hisham Cholakkal, Fahad Shahbaz Khan, Yanwei Pang, and Ling Shao. Sipmask: Spatial information preservation for fast image and video instance segmentation. *ECCV*, 2020.
- [10] Nicolas Carion, Francisco Massa, Gabriel Synnaeve, Nicolas Usunier, Alexander Kirillov, and Sergey Zagoruyko. End-to-end object detection with transformers. In *ECCV*, 2020.
- [11] Hao Chen, Kunyang Sun, Zhi Tian, Chunhua Shen, Yongming Huang, and Youliang Yan. BlendMask: Top-down meets bottom-up for instance segmentation. In *CVPR*, 2020.
- [12] Kai Chen, Jiangmiao Pang, Jiaqi Wang, Yu Xiong, Xiaoxiao Li, Shuyang Sun, Wansen Feng, Ziwei Liu, Jianping Shi, Wanli Ouyang, Chen Change Loy, and Dahua Lin. Hybrid task cascade for instance segmentation. In *CVPR*, 2019.
- [13] Xinlei Chen, Ross Girshick, Kaiming He, and Piotr Dollár. Tensormask: A foundation for dense object segmentation. In *ICCV*, 2019.
- [14] Yihong Chen, Yue Cao, Han Hu, and Liwei Wang. Memory enhanced global-local aggregation for video object detection. In *CVPR*, 2020.
- [15] Yinpeng Chen, Xiyang Dai, Mengchen Liu, Dongdong Chen, Lu Yuan, and Zicheng Liu. Dynamic convolution: Attention over convolution kernels. In *CVPR*, 2020.
- [16] Jifeng Dai, Kaiming He, Yi Li, Shaoqing Ren, and Jian Sun. Instance-sensitive fully convolutional networks. In *ECCV*. Springer, 2016.
- [17] Jifeng Dai, Haozhi Qi, Yuwen Xiong, Yi Li, Guodong Zhang, Han Hu, and Yichen Wei. Deformable convolutional networks. In *ICCV*, 2017.
- [18] Bert De Brabandere, Davy Neven, and Luc Van Gool. Semantic instance segmentation with a discriminative loss function. *arXiv preprint arXiv:1708.02551*, 2017.
- [19] Jiajun Deng, Yingwei Pan, Ting Yao, Wengang Zhou, Houqiang Li, and Tao Mei. Relation distillation networks for video object detection. In *ICCV*, 2019.
- [20] Alexey Dosovitskiy, Philipp Fischer, Eddy Ilg, Philip Hausser, Caner Hazirbas, Vladimir Golkov, Patrick Van Der Smagt, Daniel Cremers, and Thomas Brox. Flownet: Learning optical flow with convolutional networks. In *CVPR*, 2015.
- [21] Christoph Feichtenhofer, Axel Pinz, and Andrew Zisserman. Detect to track and track to detect. In *ICCV*, 2017.
- [22] Yang Fu, Linjie Yang, Ding Liu, Thomas S. Huang, and Humphrey Shi. Compfeat: Comprehensive feature aggregation for video instance segmentation. *AAAI*, 2021.
- [23] Golnaz Ghiasi, Tsung-Yi Lin, and Quoc V Le. Nas-fpn: Learning scalable feature pyramid architecture for object detection. In *CVPR*, 2019.
- [24] B. Graham. Spatially-sparse convolutional neural networks. *Computer Science*, 34(6), 2014.
- [25] Bharath Hariharan, Pablo Arbeláez, Ross Girshick, and Jitendra Malik. Simultaneous detection and segmentation. In *ECCV*. Springer, 2014.
- [26] Kaiming He, Georgia Gkioxari, Piotr Dollár, and Ross Girshick. Mask r-cnn. In *ICCV*, 2017.
- [27] Kaiming He, Xiangyu Zhang, Shaoqing Ren, and Jian Sun. Deep residual learning for image recognition. In *CVPR*, 2016.
- [28] Han Hu, Jiayuan Gu, Zheng Zhang, Jifeng Dai, and Yichen Wei. Relation networks for object detection. In *CVPR*, 2018.
- [29] Gao Huang, Danlu Chen, Tianhong Li, Felix Wu, Laurens van der Maaten, and Kilian Q Weinberger. Multi-scale dense networks for resource efficient image classification. *ICLR*, 2018.
- [30] Zhaojin Huang, Lichao Huang, Yongchao Gong, Chang Huang, and Xinggang Wang. Mask scoring r-cnn. In *CVPR*, 2019.
- [31] Dahun Kim, Sanghyun Woo, Joon-Young Lee, and In So Kweon. Video panoptic segmentation. In *CVPR*, 2020.
- [32] Bo Li, Wei Wu, Qiang Wang, Fangyi Zhang, Junliang Xing, and Junjie Yan. Siamrpn++: Evolution of siamese visual tracking with very deep networks. In *CVPR*, 2019.
- [33] Bo Li, Junjie Yan, Wei Wu, Zheng Zhu, and Xiaolin Hu. High performance visual tracking with siamese region proposal network. In *CVPR*, 2018.

- [34] Yanwei Li, Lin Song, Yukang Chen, Zeming Li, Xiangyu Zhang, Xingang Wang, and Jian Sun. Learning dynamic routing for semantic segmentation. In *CVPR*, 2020.
- [35] Chung-Ching Lin, Ying Hung, Rogerio Feris, and Linglin He. Video instance segmentation tracking with a modified vae architecture. In *CVPR*, 2020.
- [36] Tsung-Yi Lin, Piotr Dollár, Ross B. Girshick, Kaiming He, Bharath Hariharan, and Serge J. Belongie. Feature pyramid networks for object detection. In *CVPR*, 2017.
- [37] Tsung-Yi Lin, Priya Goyal, Ross Girshick, Kaiming He, and Piotr Dollár. Focal loss for dense object detection. In *ICCV*, 2017.
- [38] Tsung-Yi Lin, Michael Maire, Serge Belongie, James Hays, Pietro Perona, Deva Ramanan, Piotr Dollár, and C Lawrence Zitnick. Microsoft coco: Common objects in context. In *ECCV*, 2014.
- [39] Hanxiao Liu, Karen Simonyan, and Yiming Yang. Darts: Differentiable architecture search. *ICLR*, 2019.
- [40] Haotian Liu, Rafael A. Rivera Soto, Fanyi Xiao, and Yong Jae Lee. Yolactedge: Real-time instance segmentation on the edge (jetson agx xavier: 30 fps, rtx 2080 ti: 170 fps). *arXiv preprint arXiv:2012.12259*, 2020.
- [41] Shu Liu, Lu Qi, Haifang Qin, Jianping Shi, and Jiaya Jia. Path aggregation network for instance segmentation. *CVPR*, Jun 2018.
- [42] Yiding Liu, Siyu Yang, Bin Li, Wengang Zhou, Jizheng Xu, Houqiang Li, and Yan Lu. Affinity derivation and graph merge for instance segmentation. In *ECCV*, 2018.
- [43] Davy Neven, Bert De Brabandere, Marc Proesmans, and Luc Van Gool. Instance segmentation by jointly optimizing spatial embeddings and clustering bandwidth. In *CVPR*, 2019.
- [44] Seoung Wug Oh, Joon-Young Lee, Ning Xu, and Seon Joo Kim. Video object segmentation using space-time memory networks. In *ICCV*, 2019.
- [45] Adam Paszke, Sam Gross, Francisco Massa, Adam Lerer, James Bradbury, Gregory Chanan, Trevor Killeen, Zeming Lin, Natalia Gimelshein, Luca Antiga, et al. Pytorch: An imperative style, high-performance deep learning library. *arXiv preprint arXiv:1912.01703*, 2019.
- [46] Federico Perazzi, Anna Khoreva, Rodrigo Benenson, Bernt Schiele, and Alexander Sorkine-Hornung. Learning video object segmentation from static images. In *CVPR*, 2017.
- [47] Federico Perazzi, Jordi Pont-Tuset, Brian McWilliams, Luc Van Gool, Markus Gross, and Alexander Sorkine-Hornung. A benchmark dataset and evaluation methodology for video object segmentation. In *CVPR*, 2016.
- [48] Hieu Pham, Melody Guan, Barret Zoph, Quoc Le, and Jeff Dean. Efficient neural architecture search via parameters sharing. In *ICML*, 2018.
- [49] Siyuan Qiao, Yukun Zhu, H. Adam, A. Yuille, and Liang-Chieh Chen. Vip-deeplab: Learning visual perception with depth-aware video panoptic segmentation. *CVPR*, 2021.
- [50] Shaoqing Ren, Kaiming He, Ross Girshick, and Jian Sun. Faster r-cnn: Towards real-time object detection with region proposal networks. *arXiv preprint arXiv:1506.01497*, 2015.
- [51] Olga Russakovsky, Jia Deng, Hao Su, Jonathan Krause, Sanjeev Satheesh, Sean Ma, Zhiheng Huang, Andrej Karpathy, Aditya Khosla, Michael Bernstein, et al. Imagenet large scale visual recognition challenge. *IJCV*, 2015.
- [52] E. Shelhamer, K. Rakelly, J. Hoffman, and T. Darrell. Clockwork convnets for video semantic segmentation. *ECCV*, 2016.
- [53] Lin Song, Yanwei Li, Zhengkai Jiang, Zeming Li, Hongbin Sun, Jian Sun, and Nanning Zheng. Fine-grained dynamic head for object detection. In *NIPS*, 2020.
- [54] Mingxing Tan, Ruoming Pang, and Quoc V Le. Efficientdet: Scalable and efficient object detection. In *CVPR*, 2020.
- [55] Zhi Tian, Chunhua Shen, and Hao Chen. Conditional convolutions for instance segmentation. In *ECCV*, 2020.
- [56] Zhi Tian, Chunhua Shen, Hao Chen, and Tong He. FCOS: A simple and strong anchor-free object detector. *TPAMI*, 2021.
- [57] Pavel Tokmakov, Karteek Alahari, and Cordelia Schmid. Learning motion patterns in videos. In *CVPR*, 2017.
- [58] Pavel Tokmakov, Karteek Alahari, and Cordelia Schmid. Learning video object segmentation with visual memory. In *ICCV*, 2017.
- [59] Paul Voigtlaender, Yuning Chai, Florian Schroff, Hartwig Adam, Bastian Leibe, and Liang-Chieh Chen. Feelvos: Fast end-to-end embedding learning for video object segmentation. In *CVPR*, 2019.
- [60] Paul Voigtlaender, Michael Krause, Aljosa Osep, Jonathon Luiten, Berin Balachandar Gnana Sekar, Andreas Geiger, and Bastian Leibe. Mots: Multi-object tracking and segmentation. In *CVPR*, 2019.
- [61] Xinlong Wang, Tao Kong, Chunhua Shen, Yuning Jiang, and Lei Li. SOLO: Segmenting objects by locations. In *ECCV*, 2020.
- [62] Yuqing Wang, Zhaoliang Xu, Xinlong Wang, Chunhua Shen, Baoshan Cheng, Hao Shen, and Huaxia Xia. End-to-end video instance segmentation with transformers. In *CVPR*, 2021.
- [63] Zhongdao Wang, Liang Zheng, Yixuan Liu, and Shengjin Wang. Towards real-time multi-object tracking. *arXiv preprint arXiv:1909.12605*, 2019.
- [64] M. Weber, J. Xie, M. Collins, Yukun Zhu, P. Voigtlaender, H. Adam, B. Green, A. Geiger, B. Leibe, D. Cremers, Aljosa Osep, L. Leal-Taixé, and Liang-Chieh Chen. Step: Segmenting and tracking every pixel. *ArXiv*, abs/2102.11859, 2021.
- [65] Nicolai Wojke, Alex Bewley, and Dietrich Paulus. Simple online and realtime tracking with a deep association metric. In *ICIP*, 2017.
- [66] Yuxin Wu, Alexander Kirillov, Francisco Massa, Wan-Yen Lo, and Ross Girshick. Detectron2. <https://github.com/facebookresearch/detectron2>, 2019.
- [67] Zhenbo Xu, Wei Zhang, Xiao Tan, Wei Yang, Huan Huang, Shilei Wen, Errui Ding, and Liusheng Huang. Segment as points for efficient online multi-object tracking and segmentation. In *ECCV*, 2020.
- [68] Brandon Yang, Gabriel Bender, Quoc V Le, and Jiquan Ngiam. Condconv: Conditionally parameterized convolutions for efficient inference. *NIPS*, 2019.

- [69] Linjie Yang, Yuchen Fan, and Ning Xu. Video instance segmentation. In *ICCV*, 2019.
- [70] Linjie Yang, Yanran Wang, Xuehan Xiong, Jianchao Yang, and Aggelos K Katsaggelos. Efficient video object segmentation via network modulation. In *CVPR*, 2018.
- [71] Xingyi Zhou, Vladlen Koltun, and Philipp Krähenbühl. Tracking objects as points. In *ECCV*. Springer, 2020.
- [72] Xizhou Zhu, Jifeng Dai, Lu Yuan, and Yichen Wei. Towards high performance video object detection. In *CVPR*, 2018.
- [73] Xizhou Zhu, Han Hu, Stephen Lin, and Jifeng Dai. Deformable convnets v2: More deformable, better results. In *CVPR*, 2019.
- [74] Xizhou Zhu, Yujie Wang, Jifeng Dai, Lu Yuan, and Yichen Wei. Flow-guided feature aggregation for video object detection. In *ICCV*, 2017.
- [75] Xizhou Zhu, Yuwen Xiong, Jifeng Dai, Lu Yuan, and Yichen Wei. Deep feature flow for video recognition. In *CVPR*, 2017.
- [76] Zheng Zhu, Qiang Wang, Bo Li, Wei Wu, Junjie Yan, and Weiming Hu. Distractor-aware siamese networks for visual object tracking. In *ECCV*, 2018.
- [77] Barret Zoph and Quoc V Le. Neural architecture search with reinforcement learning. *arXiv preprint arXiv:1611.01578*, 2016.